

Different Shapes of Carbon Nanotubes via Water Assisted Chemical Vapor Deposition

Dr. Kahtan Kalaf Al-Khazraji

Materials Engineering Department, University of Technology, Baghdad.

Dr. Ali Hussain Ataiwi

Engineering College, University of Kufa, / Kufa.

Dr. Mayyadah S. Abed Al-Fatlawi 

Materials Engineering Department, University of Technology, Baghdad.

Email: mayyadah82@gmail

Received on:15/4/2014 & Accepted on:8/1/2015

ABSTRACT

Carbon nanotubes with different shapes have been prepared using water assisted chemical vapor deposition technique (WA-CVD). Different thicknesses of nickel layers were sputtered on alumina substrate. These were treated under high temperature (700 °C) at hydrogen gas to grow nickel nanoparticles (Ni-NPs). Tube furnace (single type), argon and acetylene gases were used for Carbon Nanotubes (CNTs) growth. The FESEM, TEM, HRTEM, Raman spectroscopy, and XRD were used for characterization of the carbon product. The results show that Water Assisted CVD produces CNTs with no trace of amorphous carbon. Nickel catalyst thicknesses (0.5,1,3,3.45,6.8,100 nm) offer different shapes of carbon nanotubes (single walled carbon nanotube, plain MWCNT, helical carbon nanotube, carbon nanofiber).

Keywords: Carbon nanotube, Water assisted CVD, Ni catalyst.

اشكال مختلفة من انابيب الكربون النانوية بطريقة ترسيب البخار الكيميائي بمساعدة الماء

الخلاصة

تم تحضير انابيب الكربون النانوية باشكال مختلفة باستخدام طريقة ترسيب البخار الكيميائي بمساعدة الماء. حيث تم ترسيب طبقات مختلفة السمك من النيكل بطريقة التذرية على اساس من الالومينا. وقد تمت معاملتها بالهيدروجين وعند درجة حرارة عالية (700 °C). حيث تم استخدام فرن انبوبي احادي و غاز الاستيلين وغاز الاركون لتنمية انابيب الكربون النانوية. وتم استخدام المجهر الالكتروني الماسح عالي الدقة والمجهر الالكتروني النافذ والمجهر الالكتروني النافذ عالي الدقة ومطياف رامان والاشعة السينية المنحادة لتشخيص الكربون الناتج. بينت

النتائج بان استخدام الترسيب البخار الكيميائي بمساعدة الماء ينتج انابيب كاربون بدون وجود اثر للكربون غير المتبلور. وان اختلاف سمك طبقة المادة المساعدة (0.5, 1, 3, 3.45, 6.8, 100 nm) اعطت اشكال مختلفة من انابيب الكاربون النانوية وهي انابيب الكاربون احادية الجدران ومتعددة الجدران المستوية والحلزونية، والياف الكاربون النانوية.

INTRODUCTION

Interest in carbon nanotubes continues to grow after the CNTs discovery by Japanese scientist; Iijima; in 1991 [1]. This interest continues to grow due to the unique characteristics of CNTs with wide range of properties which make CNTs compatible for many applications in electronics, water filtration, gas sensing, composite, hydrogen storage, medical application like drug delivery etc. [2-5].

Carbon nanotubes are large pure self-assemble crystalline carbon molecules with sp^2 hybridization with long thin cylinder structure of one atom thick sheet of carbon (graphene). Each carbon atom in graphene sheet bonds covalently with three another carbon atoms forming honey-comb hexagon network. If carbon nanotube grows from one atom thick sheet, it will form single wall carbon nanotube SWCNT, but if it grows from many layers of graphene separated by Vander Waals forces, it will form multi wall carbon nanotube MWCNT. Carbon nanotube is one member of fullerenes family with elongated mid [6]. Carbon nanotubes have very high range of properties depending on diameter (for SWCNT 1-3 nm, and 4-more than 50 nm for MWCNT), length (hundred to thousand nm), aspect ratio L/D (up to several hundred thousand) [7]. There are many different shapes of CNTs [8]. There are three main approaches to growth CNTs: arc discharge, laser ablation and chemical vapor deposition (CVD) [9&10]. Water assisted CVD is modified approach of CVD using H₂O vapor with few amount to enhance the quality of produced CNTs by increase the active life of catalyst [11,12].

Experimental Work

Carbon Nanotubes Preparation

The current work was done in Engineering College laboratories, Micro/Nano Systems & Nanotechnology Center laboratories, and Electron Microscopy Core Facility EMC/University of Missouri (MU)-Columbia/USA. In this work carbon nanotubes were prepared by water assisted CVD using the temperature-time curve in Fig. 1. Different thicknesses of nickel thin film were deposited (0.5, 1, 3, 3.45, 6.8, and 100 nm) by two different sputtering systems separately. Nickel thin films with thickness (0.5, 1 and 3) nm were deposited with DC magnetron sputtering system (AJA International sputtering systems) at different period of time (0.5, 1 and 3 min) respectively with deposition rate (1nm/min). The thin films with thickness (3.45, 6.8, and 100 nm) were deposited by DC magnetron sputtering technique (model EMS575X) at three different period of time (20, 40, and 500 sec.) respectively. Deposition conditions are: vacuum 9×10^{-2} mbar, electric current 20 mA.

The pre-coated substrates with catalyst were put inside the single tube furnace in CVD system. One end of the furnace is used for gas inlet of argon (Ar), hydrogen (H₂), water vapor and carbon source (acetylene C₂H₂). The flow rate of these gases (Ar/H₂/C₂H₂ 100/100/20 SCCM) was controlled by digital flow meter controller with high precision. Argon gas (Ar) was charged to the system from the beginning of the CVD process

reaching for (700 °C) and then cooling to room temperature. Argon acts as an inert gas, soot or amorphous carbon barrier, and water vapor carrier.

Argon gas was charged through the water bubbler which kept at (60°C). Hydrogen acts as a reduction gas of the oxides in the catalyst film. That makes the catalyst more efficient.

Characterization Techniques

FESEM (type Hitachi S-4700- FESEM, Japan), TEM (type JEOL 1400, Japan), HRTEM (type Tecnai G2F30 twin microscope S/TEM, FEI company, USA), X-Ray Diffraction type (Rigaku-Model Ultima IV, Japan), Raman spectroscopy (type Renishaw in Via, UK) were used to characterize the prepared CNTs.

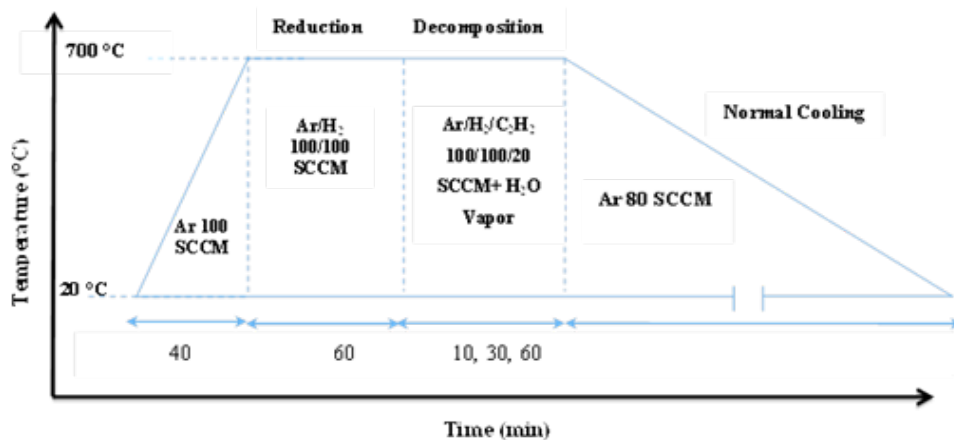


Figure 1: Temperature-time curve of WA-CVD in this Work.

Results and Discussion

One drop of sonicated (annealed catalyst or prepared CNTs and ethanol) was put on TEM grid, dried and then investigated by TEM device.

Fig. 2- Fig. 7 show TEM images of obtained Ni nanoparticles by annealing Ni thin film catalyst at 700 °C under hydrogen at different thickness (0.5, 1, 3, 3.45, 6.8, and 100 nm). It could be observed that the thin film is converted to nanoparticles. In real, after sputtering process, Ni thin film would not stay pure metal but it converts to thin film of Ni oxide. When thin film of oxide exposed to reduction gas (H₂), it would reduce to nanoparticles of pure Ni metal. Through annealing at high temperatures the reduced atoms in each crystal rearrange themselves and grow as nanoparticles. The difference in thermal expansion coefficient between the substrate and the metallic film induces stresses that relax by breaking the film in small islands. Controlling the initial thickness of the film and the reduction time and temperature, it is possible to tune the size of the nanoparticles [13,14].

It was also observed from these figures that the nanoparticles size depends on the thin film thickness that means the thicker thin film gives the bigger nanoparticles. The obtained nanoparticles average size are (3, 5, 21, 26, 67, and 510 nm) from thin film thicknesses (0.5, 1, 3, 3.45, 6.8, and 100 nm) respectively. The average size of

nanoparticles was calculated using Image J program. Fig. 8 shows the relationship between the thin film thickness and particle size of nanoparticles of nickel.

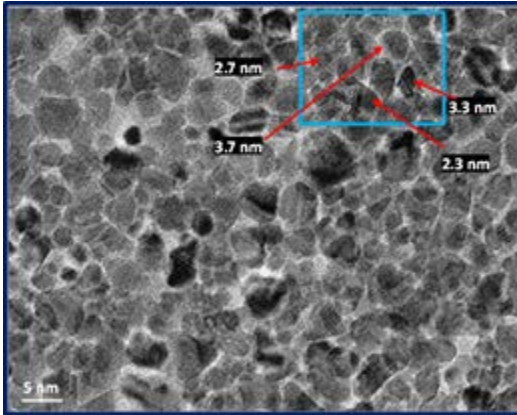


Figure 2: HRTEM image of Ni nanoparticles after annealing (0.5 nm Ni thin film).

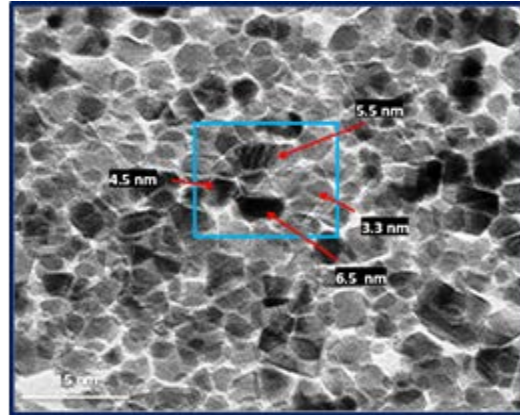


Figure 3: TEM image of Ni nanoparticles after annealing (1 nm Ni thin film).

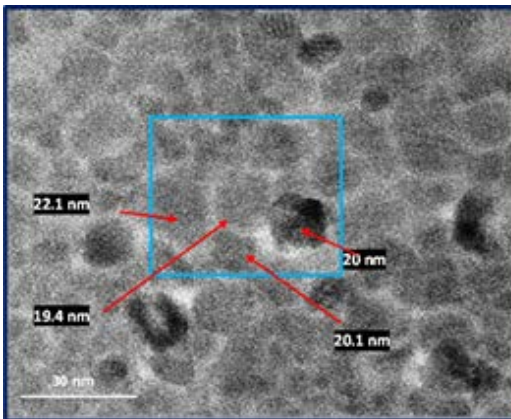


Figure 4: TEM image of Ni nanoparticles after annealing (3 nm Ni thin film).

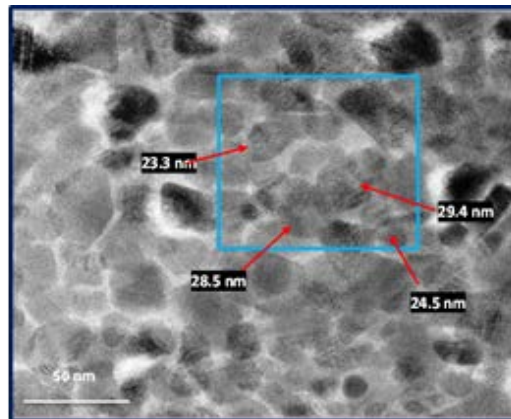


Figure 5: TEM image of Ni nanoparticles after annealing (3.45 nm Ni thin film).

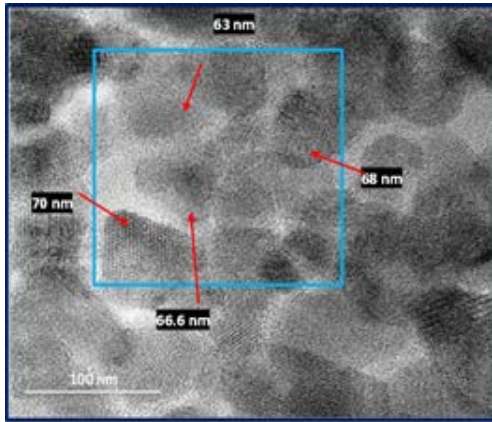


Figure 6: TEM image of Ni nanoparticles after annealing (6.8 nm Ni thin film).

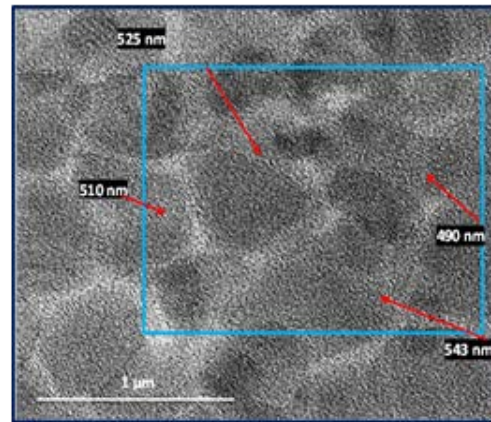


Figure 7: TEM image of Ni nanoparticles after annealing (100 nm Ni thin film).

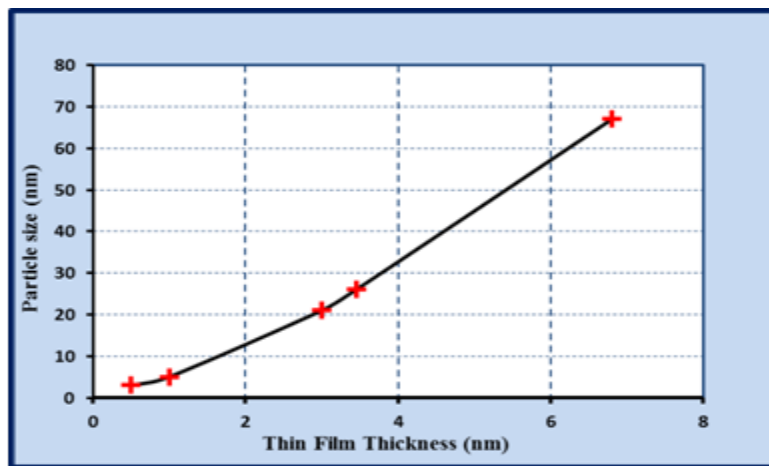


Figure 8: Relationship between the particle sizes of nanoparticles and the thin film thickness of Ni catalyst.

Fig. 9 and Fig. 10, show the FESEM and TEM and HRTEM images of Single-Walled Carbon Nanotubes SWCNTs that were grown using (0.5 and 1 nm) Ni thin film thicknesses respectively. It could be noticed that the obtained average diameter of carbon nanotubes depends on the catalyst thickness from which they grown.

Fig. 11 - Fig. 13 show the FESEM, TEM and HRTEM images of CNTs that grown from Ni catalyst thicknesses (3, 3.45, and 6.8 nm) respectively. Multi-Walled Carbon Nanotubes MWCNTs are shown distinctively in these figures. It could be observed the broadening of CNTs average diameter with size (20-88) nm. This occurs due to the difference in thermal expansion coefficient between the substrate and the metallic film induces stresses that relax by breaking the film in small islands. Controlling the initial

thickness of the film, reduction time and temperature, it is possible to tune the size of the nanoparticles [15,16,17].

It could be observed from the Fig. 11 - Fig. 13, two types of MWCNTs: Plain Multi-Walled Carbon Nanotubes PMWCNT and Helical Multi-Walled Carbon Nanotubes HMWCNTs or HCNTs. It was observed that PMWCNTs were grown from Ni thin film (3, and 3.45 nm), whereas HMWCNTs were grown from Ni thin film (6.8 nm). The HCNTs structure occurs due to the defects on CNTs surface. These defects are pentagon and heptagon carbon network defects instead of hexagon in graphite sheet due to the saturation at high temperature. Helical MWCNT derived from that of straight nanotubes. However, it contains defects that give rise to the twisting [18]. These defects are known as a Stone–Wales defect or Stone–Thrower–Wales defects. They are crystallographic defects that occur on carbon nanotubes and graphene due to the rearrangement of the six-membered rings of graphene into pentagons and heptagons[19,20,21].

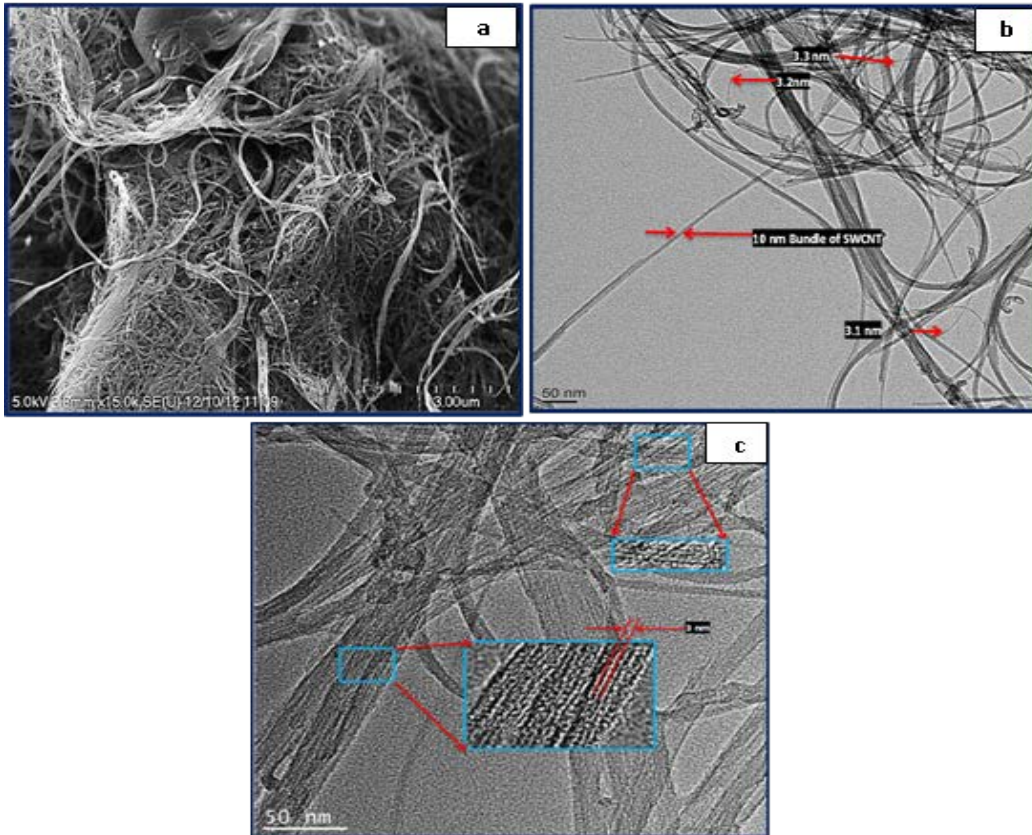


Figure 9: SWCNTs which are grown from 0.5 nm Ni thin film after annealing, a) Secondary electron image of SWCNTs bundle by HRSEM, b) TEM image of SWCNTs, and c) HRTEM image.

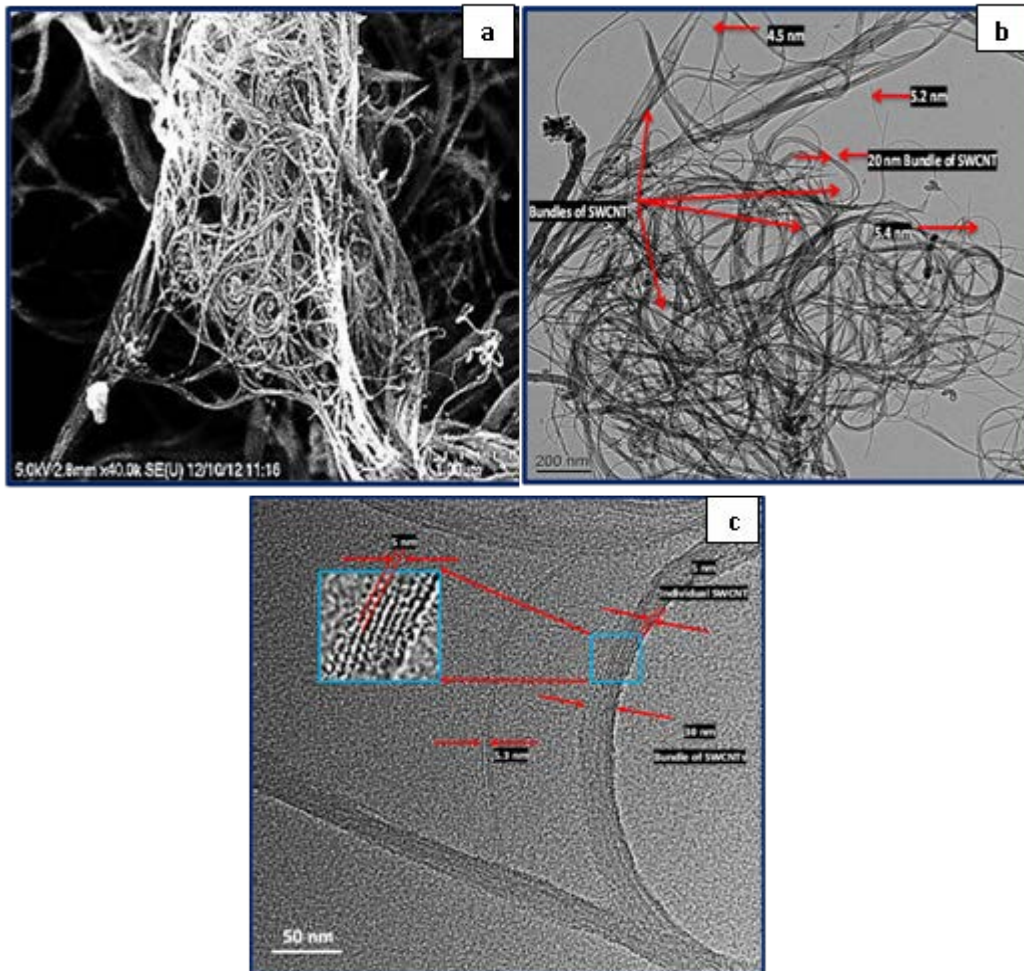


Figure 10: SWCNTs which are grown from 1 nm Ni thin film after annealing a) Secondary electron image of SWCNTs bundle by FESEM, and b) TEM image, and c) HRTEM image.

Fig. 14 shows the FESEM and HRTEM images of Carbon Nanofiber (CNF) which were grown from annealed 100 nm Ni thin films. This fiber was grown due to the large size of Ni-NPs (more than 540 nm). The obtained fiber is not hollow like CNT and with average diameter size (2-3 μm).

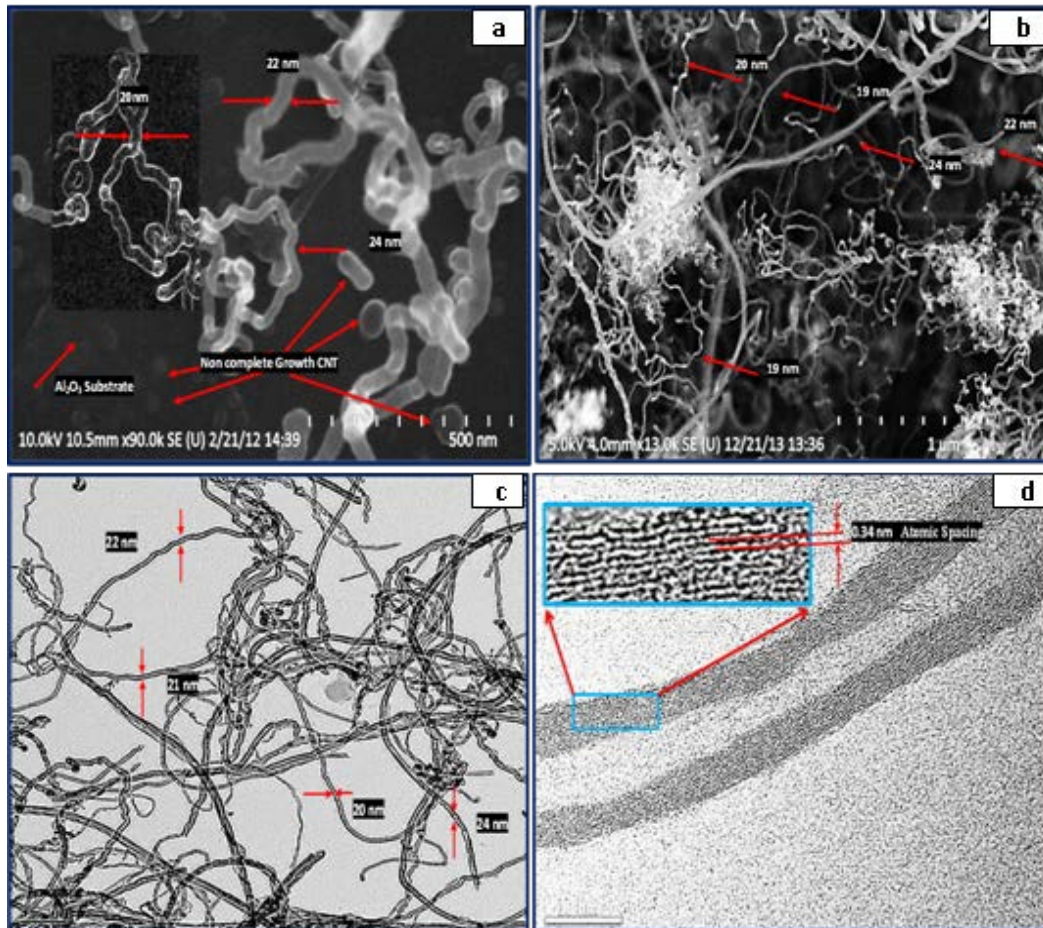


Figure 11: MWCNTs which are grown from 3 nm Ni thin film after annealing a) and b) Secondary electron images by FESEM, c) Bright field TEM image, and d) Bright field HRTEM image.

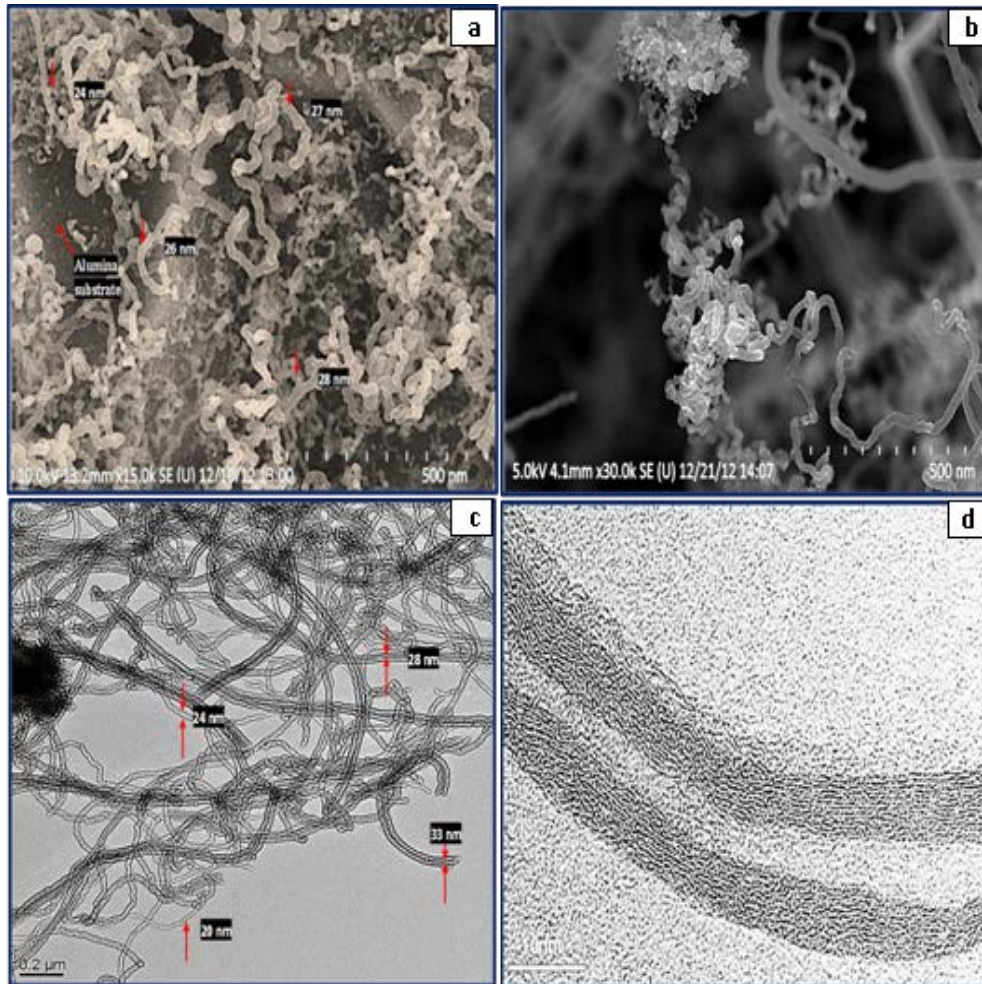


Figure 12: MWCNTs which are grown from 3.45 nm Ni thin film after annealing, a) and b) Secondary electron images by FESEM, c) Bright field TEM image, and d) Bright field HRTEM image.

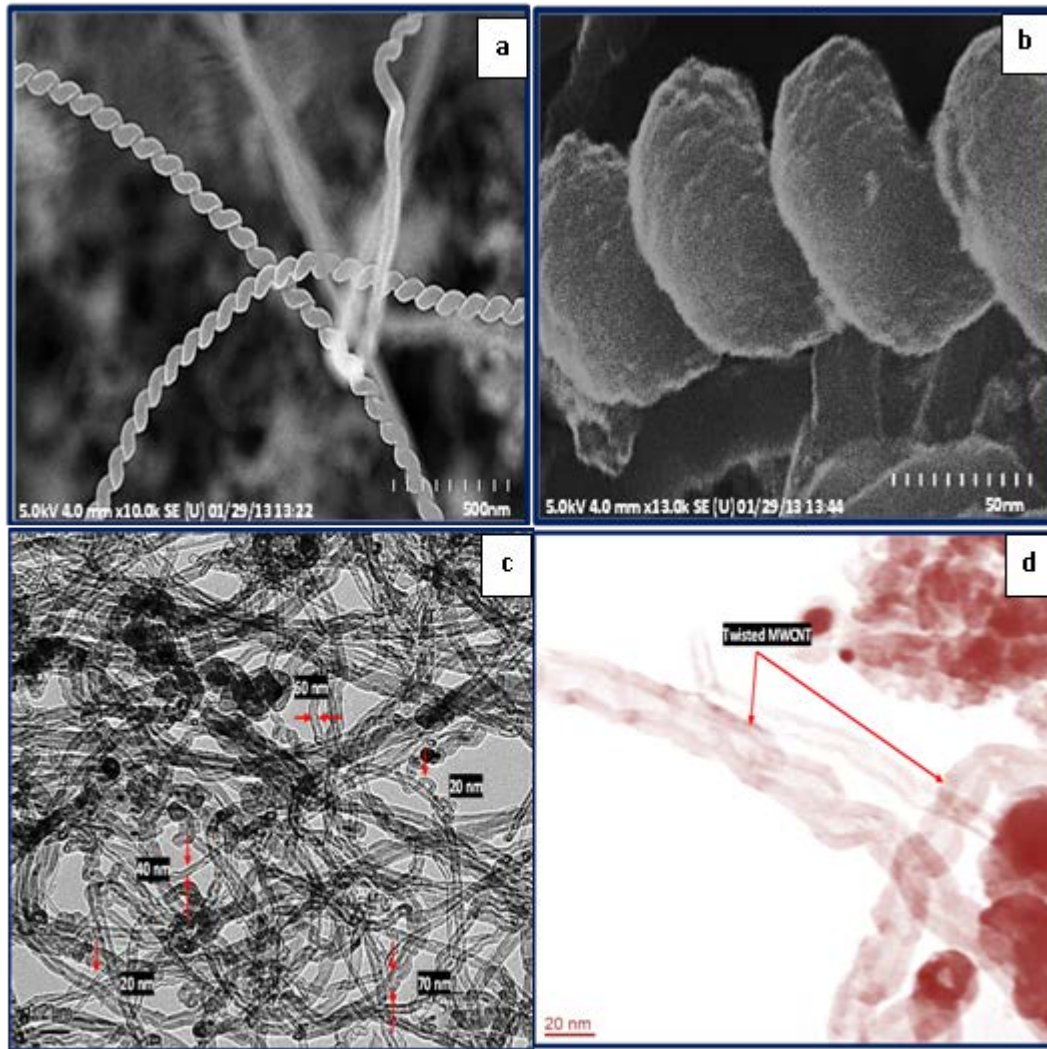


Figure 13: Helical MWCNTs which are grown from 6.8 nm Ni thin film after annealing, a) Secondary electron images FESEM, b) FESEM image at high magnification c) TEM image, and d) Low magnification HRTEM image.

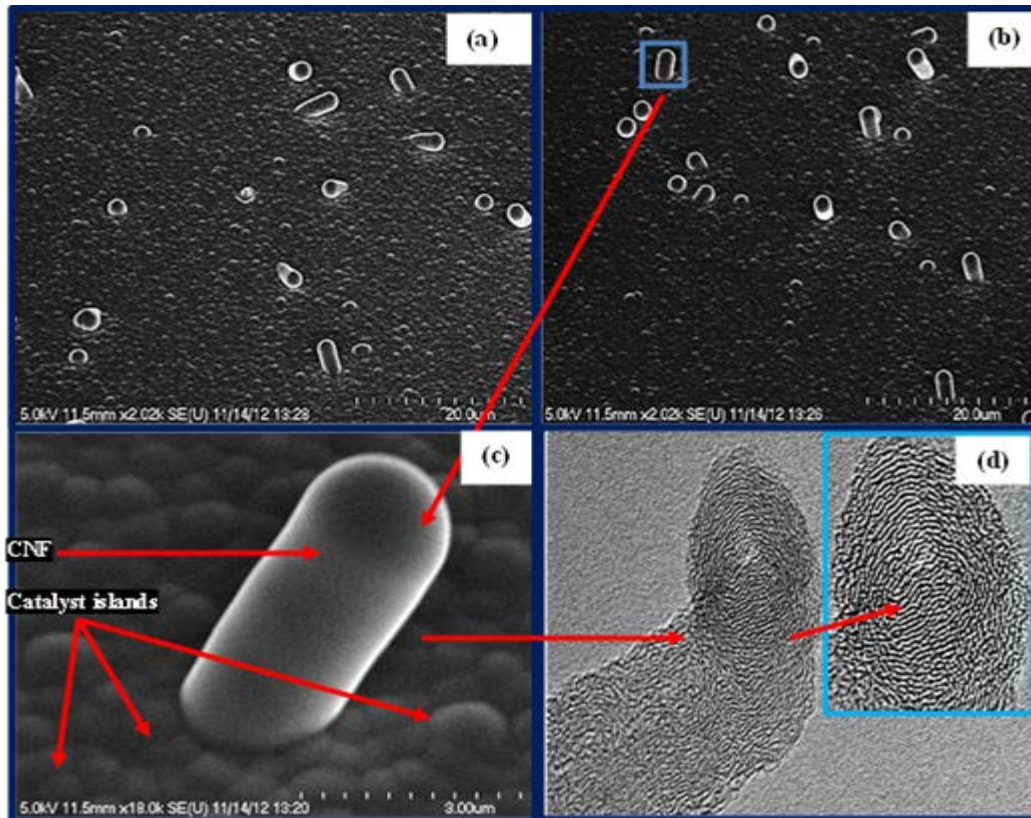


Figure 14: CNFs which are grown from 100 nm Ni thin film and 10 min growth time, a - c) Secondary electron images FESEM with different magnification, and d) HRTEM image.

The XRD pattern of the CNTs samples; were shown previously in Fig. 9 (SWCNT) and Fig. 11 (MWCNT); are shown in Figs. 15 and 16 respectively. Fig. 15 (for SWCNTs sample) displays strong broadened characteristics peak at (26.349°) and corresponding to the $(0\ 0\ 2)$ diffracting plane with d-spacing $(3.3797\ \text{\AA})$. The other peak at (42.8877°) is due to the reflection of the plane (100) , with d-spacing $(2.1075\ \text{\AA})$. Fig. 16 (for MWCNTs sample) displays a sharp characteristics peak at (25.864°) corresponding to the $(0\ 0\ 2)$ diffracting plane with d-spacing $(3.442\ \text{\AA})$. This reflecting plane (002) represents the parallel hexagon network planes in graphene sheet, and d-spacing value $(3.442\ \text{\AA})$ are the distances between adjacent two graphene layers which parallel with CNTs axis and have the strongest peaks. The other peaks at $(42.8877^\circ, 44.305^\circ, 51.718^\circ$ and $76.361^\circ)$ are due to the reflection of other planes $(100), (101), (004)$ and (101) with d-spacing $(2.1075\ \text{\AA}, 1.7661\ \text{\AA}, 1.2462\ \text{\AA},$ and $1.2462\ \text{\AA})$ respectively according to the JCPDS-ICDD cards [22,23].

The Raman shift spectra of the samples; were shown previously in Fig. 9 (SWCNT) and Fig. 11 (MWCNT); are shown in Fig. 17. The both spectra (a and b) show Defect

mode (D), Graphite mode G, and G' modes at 1360 cm^{-1} , 1580 cm^{-1} , and 2750 cm^{-1} respectively, but the Radial Breathing Mode (RBM) appears at 300 cm^{-1} for (b-spectrum) which characterize the SWCNT than MWCNT [24]. It could be observed distinctly that (I_D/I_G) ratios of CNTs are (0.413 and 0.625) for SWCNT and MWCNT respectively. MWCNT (a-spectrum) shows the lowest ratio, consequently higher quantity of structural defects due to its multiple graphite layers, whereas SWCNT (b-spectrum) shows a higher difference between D and G band.

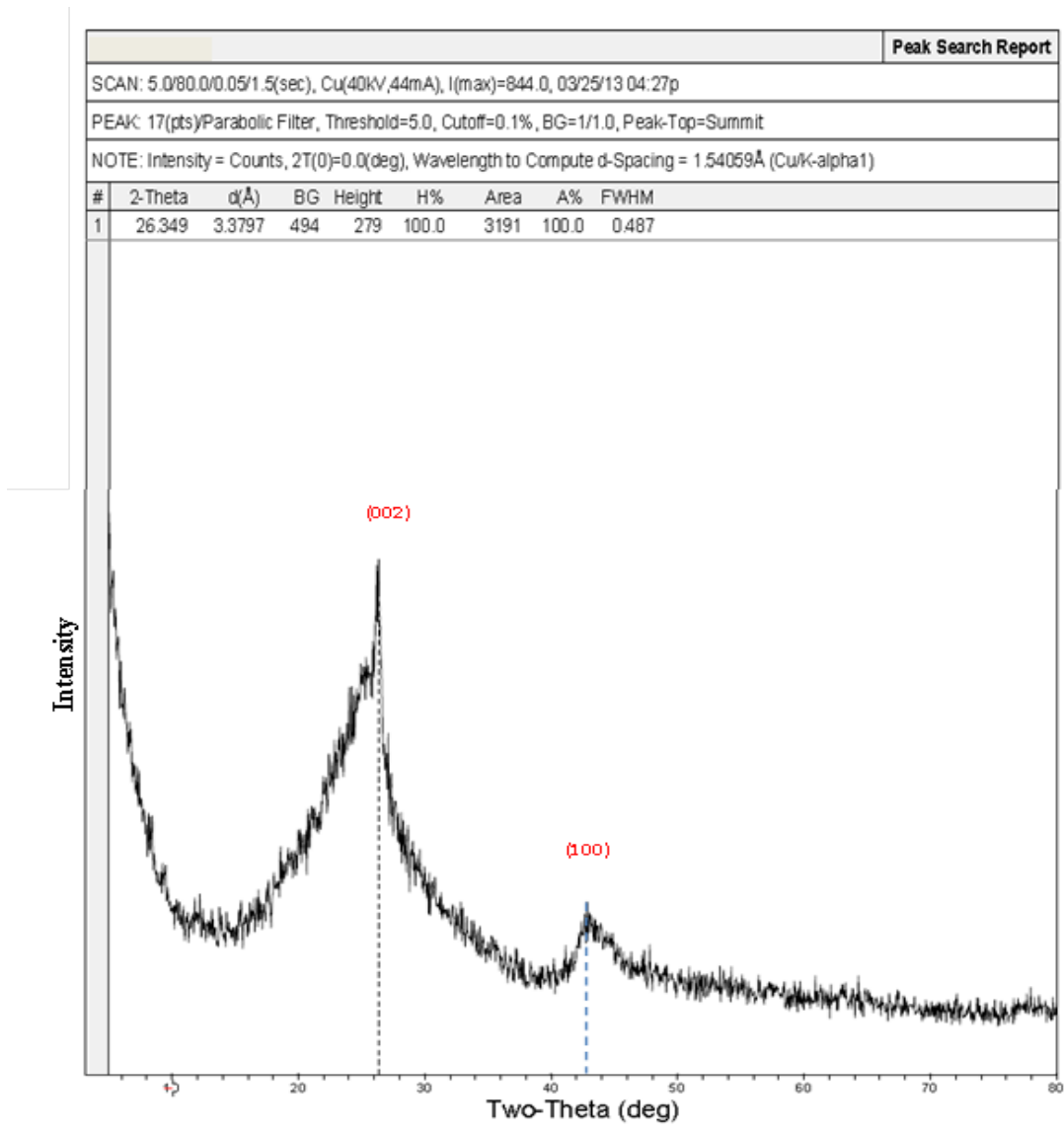


Figure 15: XRD pattern of SWCNTs.

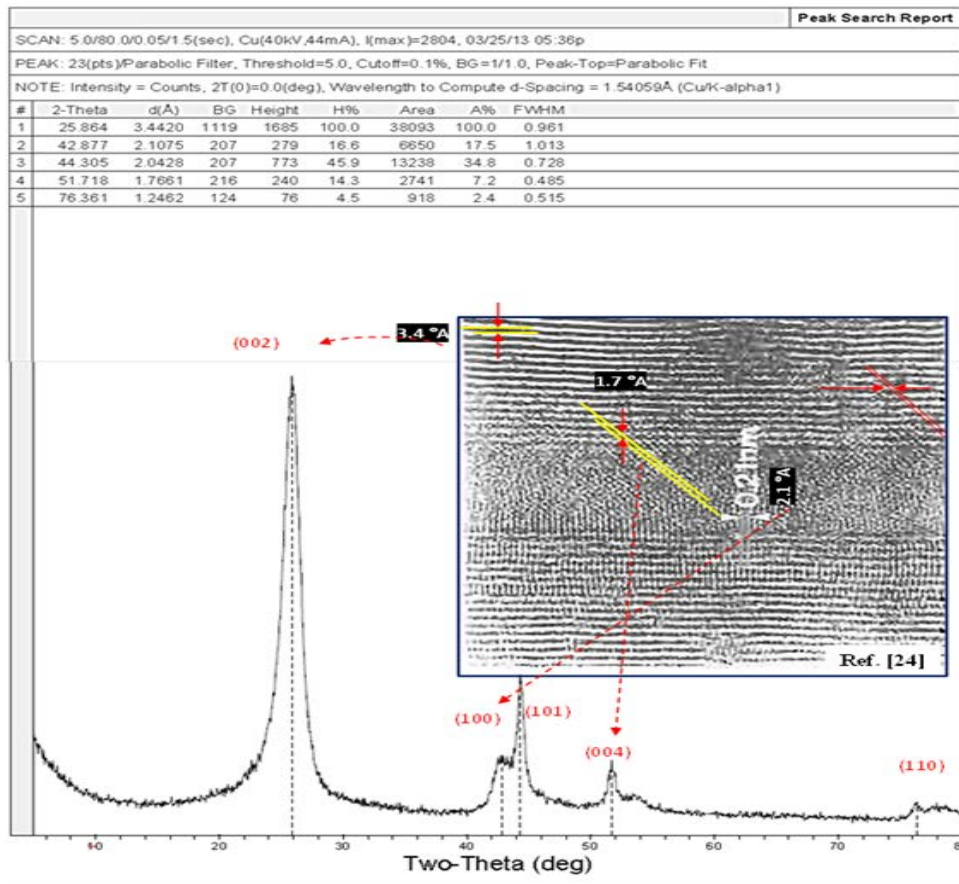


Figure 16: XRD pattern of MWCNTs.

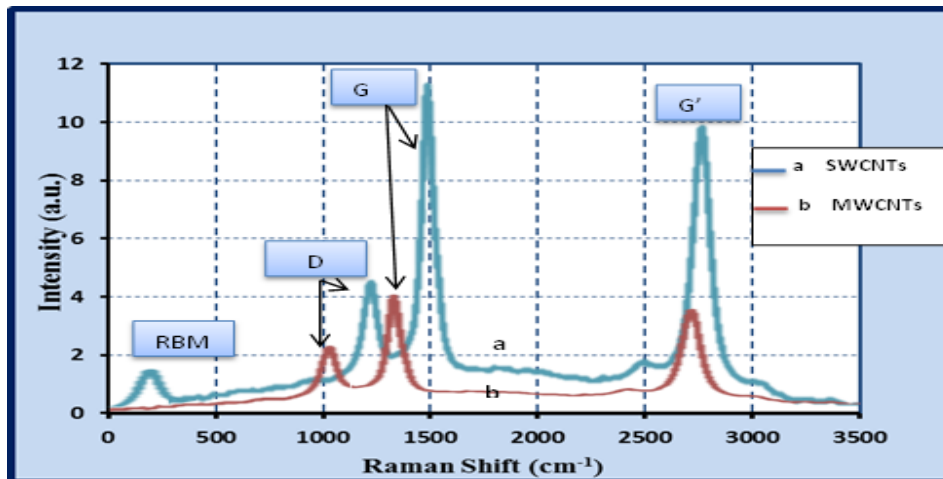


Figure 17: Raman shift spectra of CNTs.

CONCLUSION

Water assisted CVD is more efficient process to grow CNTs and prevents amorphous carbon growth when added in a suitable vapor/gases ratio (Ar/H₂/C₂H₂ 100/100/20 SCCM). Average diameters of the prepared CNTs are decreased with the decreasing of the Ni catalyst layer thickness (100, 6.8, 3.45, 3, 1, 0.5 nm). The film thickness (0.5-1 nm) encourages the SWCNTs growth rather than MWCNTs. Also the film thickness (3-3.45 nm) encourages the plain MWCNT growth rather than helical MWCNTs, whereas helical structure multi-walled carbon nanotubes HMWCNT could be obtained from Ni film thickness (6.8 nm). Finally, the thick Ni catalyst layer (around 100 nm) encourages the Carbon Nanofiber (CNFs) growth rather than CNTs.

References

- [1] Iijima, S., "Helical Microtubules of Graphitic Carbon"; *Nature*, Volume 354, pp. (56-58), (1991).
- [2] Eatemadi1, A., Daraee1, H., Karimkhanloo, H., Kouhi, M., Zarghami, N., Akbarzadeh, A., Abasi, M., Hanifehpour, Y. and Joo, S. W., "Carbon Nanotubes: Properties, Synthesis, Purification, and Medical Applications", *Nanoscale Research Letters*, Vol. 9, No.393,(2014).
- [3] Wu, H., Chang, X., Liu, L., Zhao, F., Zhao, Y., "Chemistry of Carbon Nanotubes in Biomedical Applications", *J. Mater. Chem.*, Vol. 20, pp. (1036–1052), (2010).
- [4] Valcàrcel, M., Càrdenas, S., Simonet, B.M., Moliner-Martínez, Y., Lucena, R., "Carbon Nanostructures as Sorbent Materials in Analytical Processes", *TrAC Trends Anal. Chem.*, Vol. 27, pp. (34–43), (2008).
- [5] Masotti, A. and Caporali, A. "Preparation of Magnetic Carbon Nanotubes (Mag-CNTs) for Biomedical and Biotechnological Applications" *International Journal of Molecular Sciences*, *Int. J. Mol. Sci.*, Vol. 14, pp. (24619-24642), (2013).
ISSN 1422-0067
DOI:10.3390/ijms141224619.
- [6] Burchell, T. D. "Carbon Materials for Advanced Technologies", Published by Elsevier, (1999).
- [7] Moosa, A. A. "Carbon Nanotubes: Synthesis and Applications", Dar Djlal Publishing, Amman, Jordan, (2012).
- [8] Nakayama Y. and Zhang, M., "Synthesis of Carbon Nanochaplets by Catalytic Thermal Chemical Vapor Deposition", *Japanese Journal of Applied Physics Part 2-Letters*, (JPN J A P 2), Vol. 40, No. 5B, pp. (L492-L494), (2001).
- [9] Lee, C. J., Lyu, S. C., Cho, Y. R., Lee, J. H., and Cho, K. I., "Diameter-Controlled Growth of Carbon Nanotubes Using Thermal Chemical Vapor Deposition," *Chemical Physics Letters*, Vol. 341, No. 3-4, pp. (245–249), (2001).
- [10] Thostenson, E. T., Ren, Z., and Chou, T. W., "Advances in The Science and Technology of Carbon Nanotubes and Their Composites: A Review," *Composites Science and Technology*, Vol. 61, No. 13, pp. (1899–1920), (2001).
- [11] Hata, K., Futaba, Don N., Mizuno, K., Namai, T., Yumura, M., and Iijima, S., "Water-Assisted Highly Efficient Synthesis of Impurity-Free Single-Walled Carbon Nanotubes", *SCIENCE*, Vol. 306, No. 5700, pp. (1362-1364), (2004).

- [12] Yu, M., Zhang, Y., Zeng, Y., Sadeeq, M. B., Mai, K., Zhang, Z., and Lu X., Y. Tong, "Water Surface Assisted Synthesis of Large-Scale Carbon Nanotube "Film for High-Performance and Stretchable Supercapacitors", WILEY-VCH Verlag GmbH & Co. KGaA, Weinheim, Vol. 26, No. 27, pp. (4597–4747), (2014).
DOI: 10.1002/adma.201401196
- [13] Wang, Y., Luo, Z., Li, B., Ho, P. S., Yao, Z., Shi, L., Bryan, E. N., Nemanich, R. J., "Comparison Study of Catalyst Nanoparticle Formation and Carbon Nanotube Growth: Support Effect", Journal of Applied Physics, Vol. 101, No.124310, pp. (1-8), (2007).
- [14] Serrano, A. and Garcia, M. A., "Fabrication and Incorporation of Plasmonic Nanoparticles in Macroscopic Devices", J. appl. Phys., Vol. 108, pp. 074303, (2010).
- [15] Hiramatsu, M., and Hori, M., "Aligned Growth of Single-Walled and Double-Walled Carbon Nanotube Films by Control of Catalyst Preparation", (2011), Carbon Nanotubes - Synthesis, Characterization, Applications, Dr. Yellampalli, S. (Ed.), Published by INTECH, (2011).
- [16] Huh, Y., Green, M.L.H., Kim, Y.H., Lee, J.Y. & Lee, C.J., "Control of Carbon Nanotube Growth Using Cobalt Nanoparticles as Catalyst", Applied Surface Science, Vol. 249, pp. (145–150), (2005).
- [17] Zhang, L., Tan, Y., and Resasco, D. E., "Controlling the Growth of Vertically Oriented Single-Walled Carbon Nanotubes by Varying the Density of Co-Mo Catalyst Particles", Chemical Physics Letters, Vol. 422, Issues (1–3), pp. (198–203), Published by Elsevier, (2006).
DOI: 10.1016/j.cplett.2006.02.063
- [18] Krueger, A., "Carbon Materials and Nanotechnology", Published by WILEY-VCH Verlag GmbH & Co. KGaA, Weinheim, Germany, ISBN: 978-3-527-31803-2, (2010).
- [19] Stone, A. J. and Wales, D. J., "Theoretical Studies of Icosahedral C₆₀ and Some Related Structures", Chemical Physics Letters, Vol. 128, No. (5-6), pp. (501–503), (1986).
DOI: 10.1016/0009-2614(86)80661-3
- [20] Thrower, P.A., "Chemistry and Physics of Carbon", Vol. 25, published by Marcel Dekker Inc., (1997).
- [21] Thrower, P.A., "The Study of Defects in Graphite by transmission electron microscopy", Chemistry and Physics of Carbon, Vol. 5, pp. (217–320), (1969).
- [22] JCPDS-ICDD No. 01-0640; Joint Committee on Powder Diffraction Standards-International Center for Diffraction Data of graphite, (2011).
- [23] JCPDS-ICDD No. 58-1638; Joint Committee on Powder Diffraction Standards-International Center for Diffraction Data of Carbon Nanotubes, (2011).
- [24] Tanaka, K., Yamabe, T., and Fukui, K., "The Science and Technology of Carbon Nanotubes", Published by Elsevier, (1999).